The Asymptotic Decider: Resolving the Ambiguity in Marching Cubes

Gregory M. Nielson Bernd Hamann

Computer Science
Arizona State University
Tempe, AZ 85287-5406

Abstract

A method for computing isovalue or contour surfaces of a trivariate function is discussed. The input data are values of the trivariate function, F_{ijk}, at the cuberille grid points (x_i, y_j, z_k) and the output is a collection of triangles representing the surface consisting of all points where F(x, y, z) is a constant value. The method described here is a modification that is intended to correct a problem with a previous method.

1.0 Introduction

The purpose of this paper is to describe a method for computing contour or isovalue surfaces of a trivariate function F(x, y, z). It is assumed that the function is continuous and that samples over a cuberille grid (see Figure 1) are available. These values are denoted by $F_{ijk} = F(x_i, y_j, z_k)$; i = 1, ... , Nx, j = 1, ... , Ny, k = 1, ... , Nz. The problem is to compute the isovalue or contour surface

$$S_\alpha = \{ (x, y , z) : F(x, y, z) = \alpha\}.$$

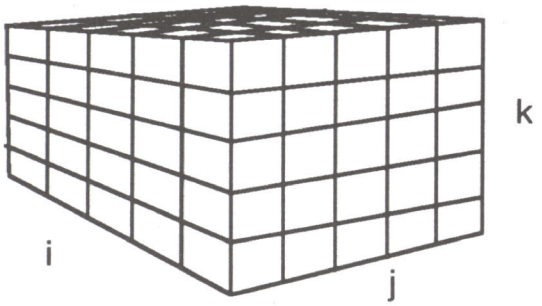

Figure 1. Cuberille Grid Data

The "marching cubes" method (hereafter referred to as mc method) produces a surface consisting of triangles whose vertices are on the edges of the voxels of the cuberille grid. The method processes one voxel at a time. The values, F_{ijk}, and linear interpolation are used to determine where the isovalue surface intersects an edge. How the intersection points are assembled into triangles depends upon the number and configuration of the grid points with values above or below the isovalue, α. The various configurations are shown in Figure 2, where a grid point that is marked indicates $F_{ijk} > \alpha$. While there are $2^8 = 256$ possible configurations, there are only 15 shown in Figure 2. This is because some configurations are equivalent with respect to certain operations. First off, the number can be reduced to 128 by assuming two configurations are equivalent if marked grid points and unmarked grid points are switched. This means that we only have to consider cases where there are four or fewer marked grid points. Further reduction to the 15 cases shown is possible by equivalence due to rotations.

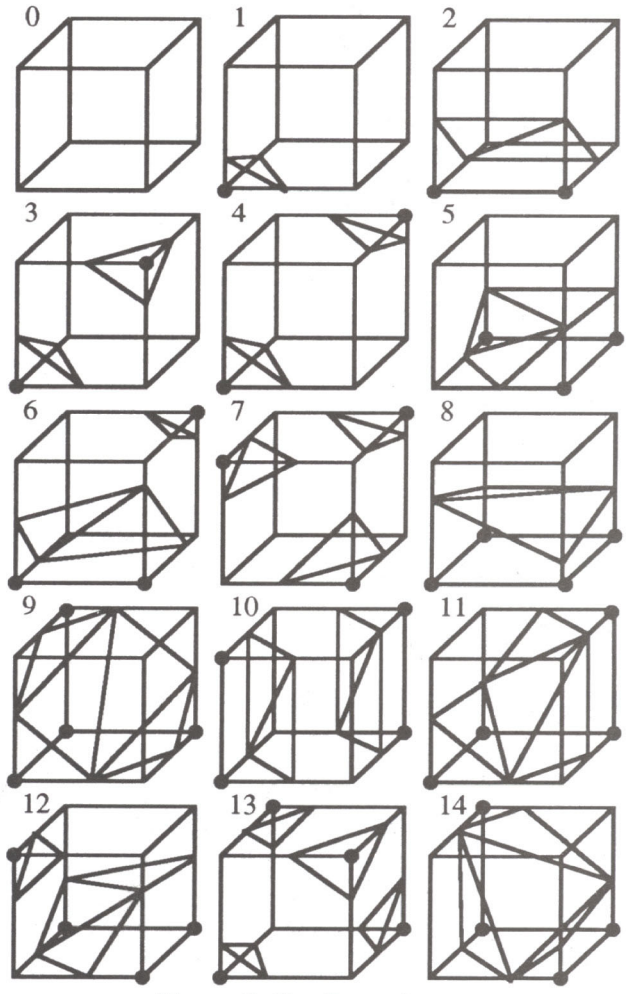

Figure 2. Configurations.

Without modification, the mc method can produce some erroneous results consisting of isosurfaces with "holes". Such a possibility is shown in Figure 3 where a voxel with configuration 6 shares a face with the complement of configuration 3. Since the line joining the upper-left-rear grid point of configuration 6 and the lower-right-front grid point of the complement of configuration 3 has one endpoint marked and the other unmarked, this line should pass through the isovalue surface. Dürst[4] points out this problem and states that the two triangles making up the quadrilateral (the 4 intersection points along the edges) on the common face should be part of the isovalue surface. We do not agree since this could lead to more than two triangles sharing a common edge. The approach presented here corrects this problem, but not in this manner. Rather, different triangulations are used. For the case at hand, there are two ways to correct the problem and both are shown in Figure 4. What distinguishes these two possibilities is the choice of the pairwise connection of the four vertices on the common face. We call such a face containing four vertices of the isovalue surface an **ambiguous face**. It is this ambiguity which is the root of the problem for the mc method. The connection of the isosurface points on the common face is done in one manner as the face of one voxel and in another manner as the face of the adjoining voxel. Any correct method needs to be consistent and in order to be consistent on these faces, different triangulations (not considered in the original mc method) must be used. As long as a consistent choice is made and a proper triangulation is used, a topologically correct surface will result. A consistent choice could be completely arbitrary, but it would be preferred if there were some reasonable basis for the choice. In the next section, we describe a technique for making this choice which is based upon bilinear variation of F on an ambiguous face. In Section 3, we discuss the modifications of the configurations of Figure 2 so as to produce a topologically correct isovalue surface. Section 4 is devoted to some examples and concluding remarks.

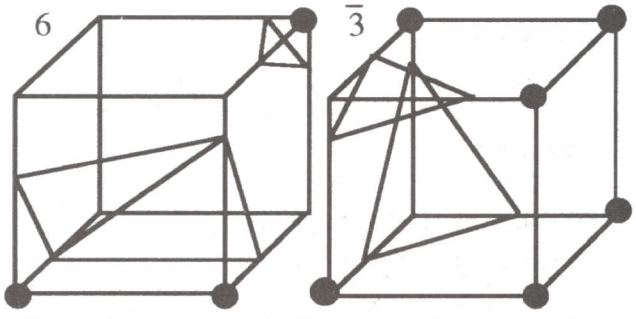

Figure 3. An example illustrating the flaw in the marching cubes method.

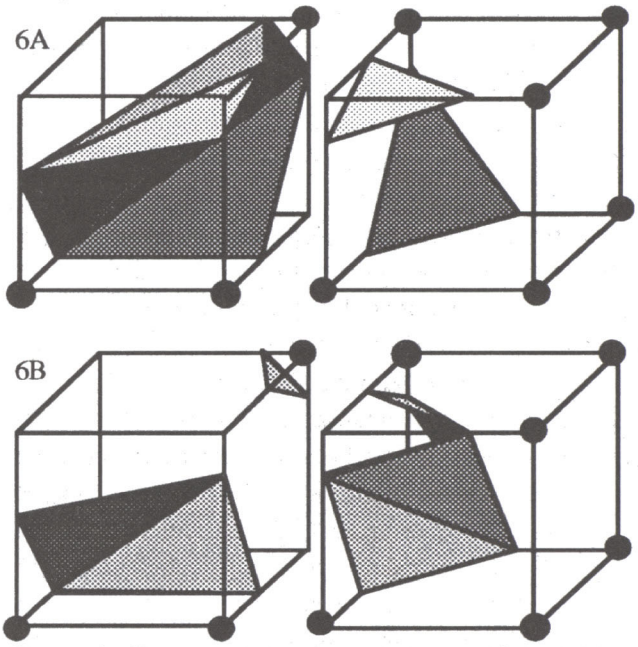

Figure 4. Two possible triangulations which yield a topologically correct isovalue surface.

2.0 Asymptotic Decider

In this section, we describe a technique for making the choice as to which vertices to connect on an ambiguous face. It is motivated by the use of bilinear variation over this face. Bilinear variation over a face is a natural extension to linear variation along an edge. Assuming a change of variables has been done, it is sufficient to consider the face domain to be a unit square, $\{ (s,t) : 0 \le s \le 1, 0 \le t \le 1 \}$ and so we have the following formula for bilinear interpolation:

$$B(s,t) = (1-s,\ s)\begin{pmatrix} B_{00} & B_{01} \\ B_{10} & B_{11} \end{pmatrix}\begin{pmatrix} 1-t \\ t \end{pmatrix}$$

where B_{00}, B_{01}, B_{10} and B_{11} represent the appropriate values of F_{ijk} at the four corner grid points (see Figure 5).

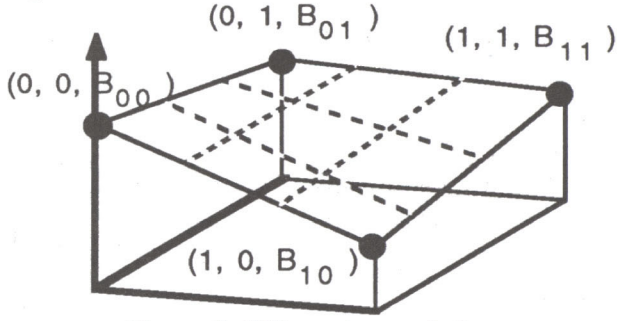

Figure 5. Bilinear interpolation.

It is easy to verify that the contour curves of B, $\{(s, t) : B(s, t) = \alpha\}$, are hyperbolas. Some

possibilities as to how these contour hyperbolas and their asymptotes relate to the domain are shown in Figure 6.

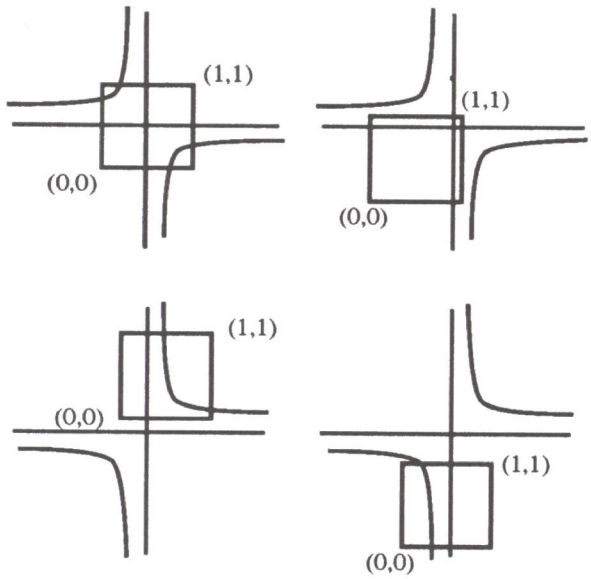

Figure 6. Contours of bilinear interpolant

The ambiguous case arises when both components of the hyperbola intersect the domain. The upper-left case of Figure 6 is such a situation. The criteria we use for connecting vertices is based upon whether or not they are joined by a component of the hyperbolic arc. As it turns out, this selection can be determined by comparing the contour value, α, with the value of the bilinear interpolant at the intersection point of the asymptotes. Based upon the notation of Figure 7, the test is:

If $\alpha > B(S_\alpha,T_\alpha)$	**then**	connect	$(S_1,1)$ to $(1,T_1)$
		and	$(S_0,0)$ to $(0,T_0)$
	else	connect	$(S_1,1)$ to $(0,T_0)$
		and	$(S_0,0)$ to $(1,T_1)$

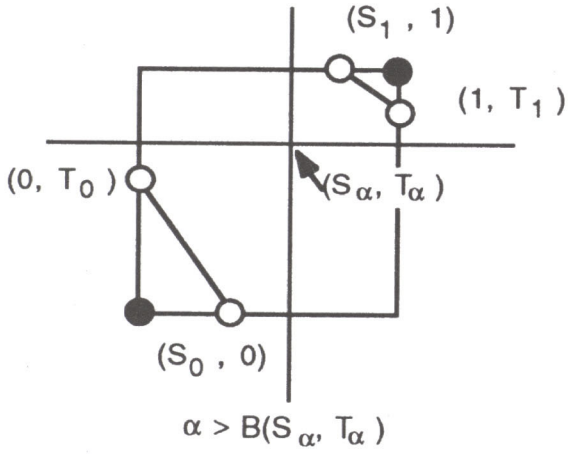

Figure 7a. Notation

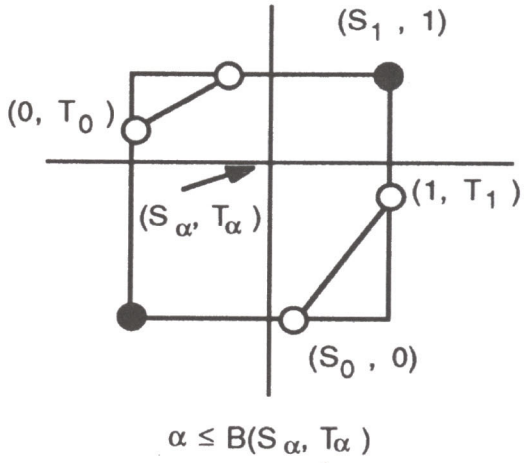

Figure 7b. Notation

The asymptotes are easy to determine. They are $\{(s, t) : s = S_\alpha\}$ and $\{(s, t) : t = T_\alpha\}$, where

$$S_\alpha = \frac{B_{00} - B_{01}}{B_{00} + B_{11} - B_{01} - B_{10}}$$

and

$$T_\alpha = \frac{B_{00} - B_{10}}{B_{00} + B_{11} - B_{01} - B_{10}}$$

Therefore, we have

$$B(S_\alpha,T_\alpha) = \frac{B_{00}\,B_{11} + B_{10}\,B_{01}}{B_{00} + B_{11} - B_{01} - B_{10}}.$$

For the subsequent discussion on how to triangulate the contours contained within a voxel which has an ambiguous face, it will be convenient to make a definition. An ambiguous face has two diagonally opposed grid points that are marked and the other two diagonally opposed grid points are unmarked. If the asymptotic decider test implies the connection of two edges common to a single marked grid point, then we say this face is **separated**; otherwise an ambiguous face is said to be **not separated**.

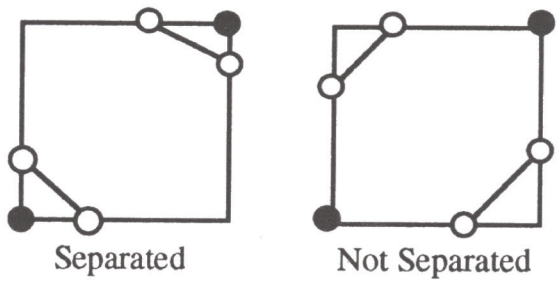

Figure 8. Ambiguous faces

3.0 The Various Cases

We now discuss the modifications necessary for the fifteen configurations of Figure 2. We first note that configurations 0, 1, 2, 4, 5, 8, 9, 11 and 14 have no ambiguous faces and so no modifications are needed for these cases. The remaining configurations need modification. Some are more complicated than others. The following discussion is roughly in order of increasing complexity. The notation is the same as for the original mc method and is shown in Figure 9.

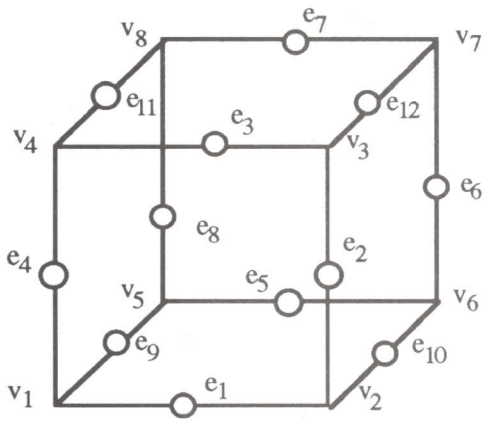

Figure 9.

Configuration 3:

This configuration has exactly one face which is ambiguous and so there are two possible ways to connect the vertices and two resulting triangulations. These are shown in Figure 10.

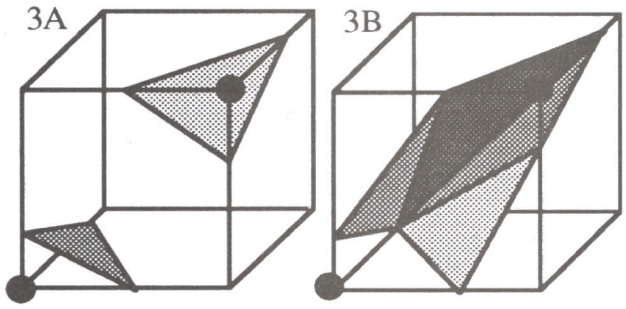

Figure 10.

Triangulations:

3A: $e_2e_3e_{12}$, $e_1e_4e_9$

3B: $e_4e_9e_3$, $e_3e_9e_{12}$, $e_9e_{12}e_2$, $e_1e_2e_9$

The reader might note that there are actually several different (and valid) triangulations of the polygon of Figure 3B. For example the "diagonal" of the quadrilateral $e_4e_3e_{12}e_9$ could be switched to replace $e_4e_9e_3$ and $e_3e_9e_{12}$ with $e_4e_3e_{12}$ and $e_4e_9e_{12}$ Whether or not this is desirable depends on the values F_{ijk} and exactly where the vertices lie on the edges. One possible criterion is discussed by Choi et al.[2].

Configuration 6:

This configuration is similar to configuration 3 in that there is only one ambiguous face; namely the right face. It differs from configuration 3 in that there are seven vertices rather than six. There are two possible triangulations which have already been shown in the left portion of Figure 4. Case B is where the right face is separated and case A is where it is not separated.

Triangulations:

6A: $e_2e_{12}e_4$, $e_4e_{12}e_7$, $e_4e_9e_7$; $e_9e_6e_7$, $e_9e_{10}e_6$

6B: $e_9e_2e_4$, $e_9e_{10}e_2$; $e_{12}e_6e_7$

Configuration 12:

For this configuration, there are two ambiguous faces; namely the front and the left. This gives rise to $2^2 = 4$ boundary polygons. Possible triangulations of these polygons are shown in Figure 11.

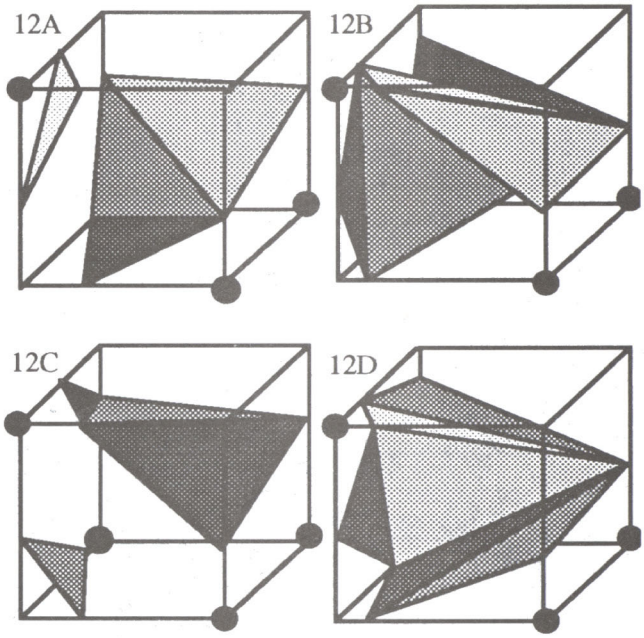

Figure 11.

Triangulations:

12A: $e_3e_{11}e_4$; $e_1e_2e_9$, $e_2e_8e_9$, $e_2e_8e_6$

12B: $e_1e_4e_{11}$, $e_6e_9e_8$, $e_1e_9e_6$, $e_1e_6e_{11}$, $e_6e_3e_{11}$, $e_6e_2e_3$

12C: $e_1e_4e_9$; $e_3e_8e_{11}$, $e_3e_6e_8$, $e_3e_2e_6$

12D: $e_3e_4e_9$, $e_6e_{11}e_8$, $e_3e_{11}e_6$, $e_3e_6e_9$, $e_6e_1e_9$, $e_6e_2e_1$

Configuration 10:

Here again we have two ambiguous faces; the top and the bottom. When both faces are separated (10A) or both are not separated (10C) there are two components for the isovalue surface. In the other two cases, where one face is separated and the other is not, the situation is quite different in that it is impossible to triangulate the boundary polygon.

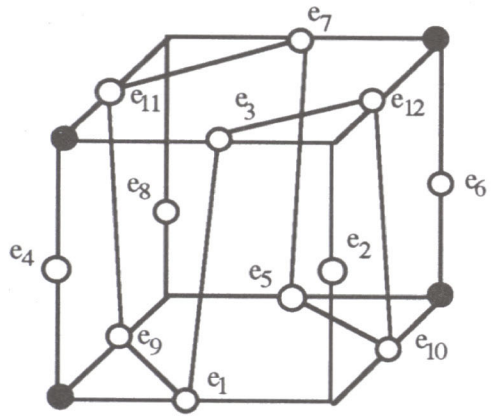

Figure 12.

In the interest of completeness, we give the following argument that the boundary polygon of Figure 12 can not be triangulated: First note that the following edges are not allowed: e_3e_{11}, e_3e_7, $e_{12}e_{11}$, $e_{12}e_7$, e_1e_{10}, e_1e_5, e_9e_{10}, e_9e_5. Now, e_9e_{11} must be the edge of some triangle. There are only two vertices that can be joined with this edge; namely e1 and e_7. Similarly, only e_3 and e_5 can join with the edge $e_{10}e_{12}$. This gives rise to four possibilities: 1) The triangles $e_3e_{12}e_{10}$ and $e_1e_9e_{11}$, 2) the triangles $e_{10}e_5e_{12}$ and $e_1e_9e_{11}$, 3) the triangles $e_{12}e_{10}e_3$ and $e_7e_{11}e_9$ 4) the triangles $e_{12}e_{10}e_5$ and $e_7e_{11}e_9$. Consider possibility 1): The edge e_1e_3 must join with some vertex to make a triangle. The only vertices left are e_{10}, e_5, e_7 and e_{11}, but if a triangle is formed with any one of these vertices, we end up with one of the disallowed edges so this is impossible. Consider possibility 2); The only vertex that can join with the edge e_5e_7 to form a triangle is e_{11}. Similarly, e_1e_3 can only join with e_{12}. Now, to complete the triangulation, we need to add either $e_{12}e_{11}$ or e_1e_5 which are both disallowed. So this is also impossible. Possibility 3 is eliminated with an argument similar to that for possibility 1 and possibility 4 is eliminated with an argument similar to that used for possibility 2. This concludes the argument.

One way to eliminate this problem of not being able to triangulate the boundary polygon is to add a vertex that is interior to the voxel. We use

$$e_0 = (1-u)e_\alpha(top) + ue_\alpha(bot)$$

where $u = \dfrac{\alpha - F(e_\alpha(top))}{F(e_\alpha(bot)) - F(e_\alpha(top))}$ and $e_\alpha(top) = (S_\alpha(top), T_\alpha(top))$, $e_\alpha(bot) = (S_\alpha(bot), T_\alpha(bot))$ are the intercepts of the asymptotes of $B(s, t) = \alpha$ on the top face and bottom face, respectively. It is easy to verify that $0<u<1$ since in each case (10B or 10D) the top and bottom differ as to whether they are separated or not.

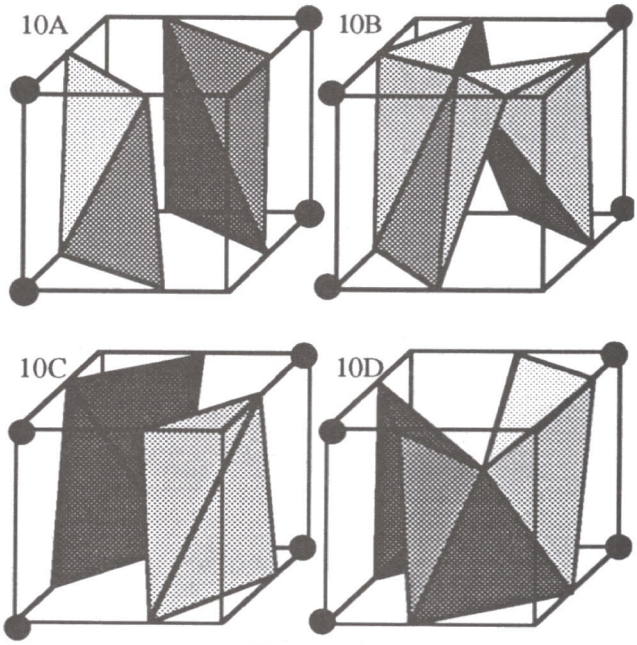

Figure 13.

Triangulations:

10A: $e_1e_3e_9$, $e_3e_9e_{11}$; $e_{10}e_{12}e_7$, $e_7e_5e_{10}$

10B: $e_1e_3e_0$, $e_3e_{12}e_0$, $e_{12}e_{10}e_0$, $e_{10}e_5e_0$, $e_5e_7e_0$, $e_7e_{11}e_0$, $e_{11}e_9e_0$, $e_9e_1e_0$

10C: $e_{11}e_7e_5$, $e_{11}e_5e_9$; $e_3e_{12}e_1$, $e_1e_{10}e_{12}$

10D: $e_1e_{10}e_0$, $e_{10}e_{12}e_0$, $e_{12}e_7e_0$, $e_7e_5e_0$, $e_5e_9e_0$, $e_9e_{11}e_0$, $e_{11}e_3e_0$, $e_3e_1e_0$

Configuration 7:

For this configuration, there are three ambiguous faces and so there are $2^3 = 8$ possibilities. These eight boundary connections are illustrated in Figure 14.

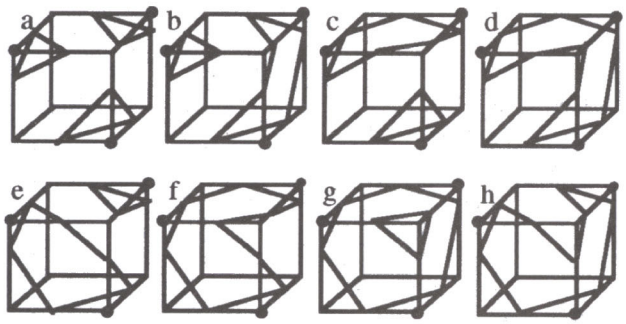

Figure 14. Eight possible boundary polygons.

Without regard to orientation, cases b, c and e are equivalent; each having two faces where the marked grid points are separated by contour edges. Cases d, f and h are also equivalent with one face where marked grid points are separated. Consequently, only four cases need be considered. The triangulations are shown in Figure 15. The case of 7C is similar to the eight point boundary polygon of configuration 10 in that an additional point is required in order to produce a valid triangulation. Here, we take this additional point e_0 to be a point on the line through grid point v_2 and grid point v_8. It is computed by linear interpolation as $e_0 = (1-u)v_2 + uv_8$ where $u = (\alpha - F(v_2)) / (F(v_8)-F(v_2))$

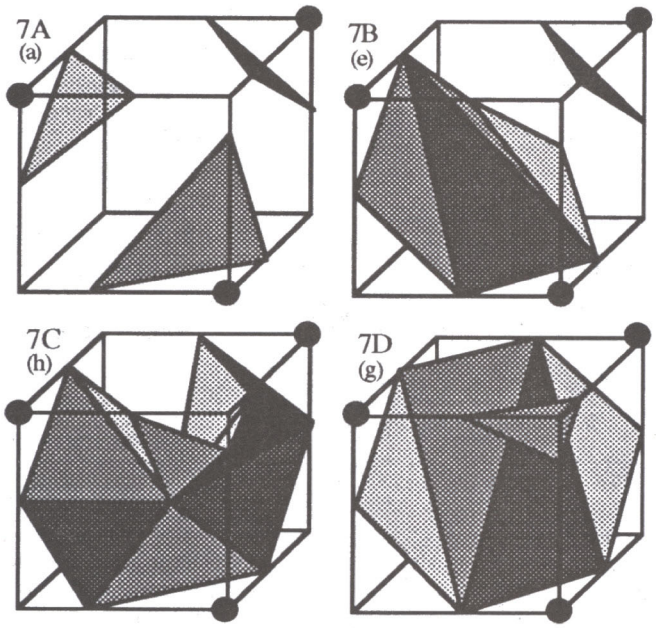

Figure 15.

Triangulations:

7A: $e_3e_4e_{11}$; $e_6e_7e_{12}$; $e_1e_2e_{10}$

7B: $e_6e_7e_{12}$; $e_{10}e_{11}e_3$, $e_{10}e_3e_2$, $e_{10}e_{11}e_1$, $e_1e_4e_{11}$

7C: $e_1e_{10}e_0$, $e_{10}e_6e_0$, $e_6e_7e_0$, $e_7e_{12}e_0$, $e_{12}e_2e_0$, $e_2e_3e_0$, $e_3e_{11}e_0$, $e_{11}e_4e_0$, $e_4e_1e_0$

7D: $e_2e_{12}e_3$; $e_{10}e_6e_7$, $e_{10}e_1e_7$, $e_1e_7e_{11}$, $e_1e_{11}e_4$

Configuration 13:

For this configuration, all six faces are ambiguous and so there are potentially $2^6 = 64$ cases to consider. This number can be reduced considerably by forming equivalence classes based upon rotations. These cases are distinguished by the number and configuration of separated faces. There can be zero separated faces up to six separated faces. In the case of two, three and four separated faces, there are two configurations each. These are all illustrated in Figure 16 except the case of six separated faces which is shown in Figure 2.

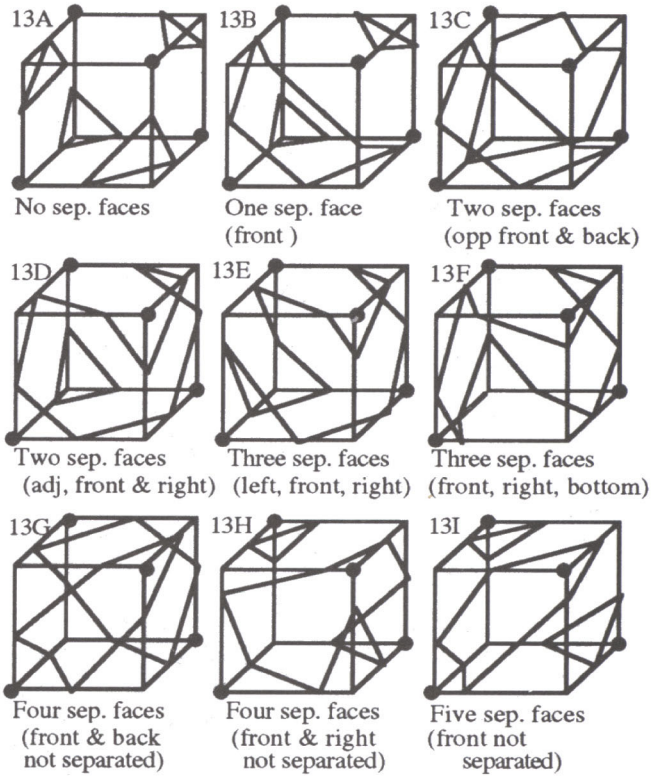

Figure 16.

The cases of 13E and 13F have a single connected boundary polygon with twelve vertices. In either case, this polygon can not be triangulated without an additional interior vertex. In the case of 13E and 13F the vertex e_0 is computed by linear interpolation on the line joining v_8 and v_2. The cases of 13D and 13H each have a boundary polygon with two components; one with three vertices and another with nine vertices. The polygons with nine vertices can not be triangulated as is. In the case of 13D an additional vertex, e_0, is taken on the line joining v_8 and v_2 and in the case of 13H, e_0, is taken on the line joining v_3 and v_5.

Triangulations:

13A: $e_3e_4e_{11}$; $e_1e_2e_{10}$; $e_5e_8e_9$, $e_6e_7e_{12}$

13B: $e_5e_8e_9$; $e_6e_7e_{12}$; $e_{10}e_{11}e_2$, $e_2e_3e_{11}$, $e_{10}e_{11}e_4$, $e_{10}e_1e_4$

13C: $e_1e_{10}e_4$, $e_{10}e_{11}e_4$, $e_{11}e_{10}e_2$, $e_2e_3e_{11}$; $e_6e_5e_{12}$, $e_{12}e_5e_9$, $e_{12}e_9e_7$, $e_7e_9e_8$

13D: $e_1e_{10}e_0$, $e_{10}e_6e_0$, $e_6e_7e_0$, $e_{12}e_7e_0$, $e_{12}e_2e_0$, $e_2e_3e_0$, $e_3e_{11}e_0$, $e_{11}e_4e_0$, $e_4e_1e_0$; $e_5e_8e_9$

13E: $e_1e_{10}e_0$, $e_{10}e_6e_0$, $e_6e_7e_0$, $e_7e_{12}e_0$, $e_{12}e_2e_0$, $e_2e_3e_0$, $e_3e_{11}e_0$, $e_{11}e_8e_0$, $e_8e_5e_0$, $e_5e_9e_0$, $e_9e_4e_0$, $e_4e_1e_0$

13F: $e_1e_9e_0$, $e_9e_8e_0$, $e_8e_5e_0$, $e_5e_{10}e_0$, $e_{10}e_6e_0$, $e_6e_7e_0$, $e_7e_{12}e_0$, $e_{12}e_2e_0$, $e_2e_3e_0$, $e_3e_{11}e_0$, $e_{11}e_4e_0$, $e_4e_1e_0$

13G: $e_1e_9e_2$, $e_9e_2e_{12}$, $e_9e_{12}e_4$, $e_4e_{12}e_3$; $e_{10}e_5e_8$, $e_{10}e_8e_{11}$, $e_{10}e_{11}e_6$, $e_6e_{11}e_7$

13H: $e_1e_9e_0$, $e_9e_4e_0$, $e_4e_3e_0$, $e_3e_{12}e_0$, $e_{12}e_6e_0$, $e_6e_5e_0$, $e_5e_{10}e_0$, $e_{10}e_2e_0$, $e_2e_1e_0$; $e_7e_{11}e_8$

13I: $e_9e_4e_3$, $e_9e_3e_{12}$, $e_9e_{12}e_1$, $e_1e_{12}e_2$; $e_{10}e_6e_5$; $e_{11}e_8e_7$

13J: $e_1e_9e_4$; $e_5e_{10}e_6$; $e_3e_2e_{12}$; $e_{11}e_8e_7$

4.0 Examples and Remarks

The modifications we have suggested for configurations with ambiguous faces adds considerable complexity to the mc method. A natural question to ask is how often do these configurations arise; if at all. The answer is that they certainly do occur in real data sets, but not very often. We have tabulated the frequency of occurrence of the various configurations for several data sets. A sample of these results is shown in Table 1. The first example consists of 69x65x65 voxels. The data is from a CAT-scan. The contour value is $\alpha = 12.6$ and Figure 17 shows the isovalue surface. The second example is over the same cuberille grid, but the values F_{ijk} are determined by evaluating the function

$$F(x,y,z) = .5\exp\{-10[(x-.25)^2 + (y-.25)^2]\} + 75\exp\{-16[(x-.25)^2 + (y-.25)^2 + (z-.25)^2]\} + .50\exp\{-10[(x-.75)^2 + (y-.125)^2 + (z-.5)^2]\} - .25\exp\{-20[(x-.75\})^2 + (y-.75)^2]\}.$$

The contour level is $\alpha = .557$. The third example uses a cuberille grid consisting of 49x49x49 voxels and the function is

$$F(x,y,z) = .7\exp\{-16[(x-.3)^2+(y-.3)^2+(z-.3)^2]\} + .9\exp\{-16[(x-.7)^2+(y-.7)^2+(z-.3)^2\} + .7\exp\{-16[(x-.3)^2+(y-.7)^2+(z-.7)^2]\} + .7\exp\{-16[(x-.7)^2+(y-.3)^2+(z-.7)^2]\}.$$

The contour level is $\alpha = .463$ and a portion of the isovalue surface using the original mc method is shown in Figure 18. The "hole" illustrates the flaw of the mc method.

Config.	Example 1	Example 2	Example 3
0	263,519	285,074	110,993
1	7,705	1,912	1,673
2	8,710	2,065	2,421
3A	60	0	6
3B	46	0	6
4	28	0	0
5	5,611	1,228	1,143
6A	20	0	0
6B	47	0	0
7A	3	0	0
7B,D	3	0	0
7C	3	0	0
8	4,637	906	1,146
9	1,003	304	261
10A,C	13	0	0
10B,D	1	0	0
11	36	0	0
12A,C	7	0	0
12B,D	4	0	0
13	0	0	0
14	69	0	0

Table 1. Frequency of configurations

Even though the ambiguous cases are infrequent, an implementation that produces correct results in all cases, must deal with them in some manner. While the modifications suggested here do add to the implementation complexity, they would not have any significant effect on the running time or the total number of triangles produced.

The approach presented here is in the spirit of repairing the mc method and is not intended to suggest that this is the preferred method of computing isovalue surfaces in all circumstances. There are other methods for solving this problem. Some are modifications of the mc method (see [2], for example) and others are based upon assembling curve contours from slices (see [1] and [7]). The method proposed by Wilhelms and Van Gelder [15] resolves this ambiguity by using estimates of gradients obtained by fitting a low degree polynomial. A very simple approach (see [13], [12], and [11]) is based upon subdividing each cube into 5 (or 6) tetrahedra and assuming linear variation on each tetrahedron. This method produces more triangles than the mc method, but if this is a problem, it is possible to "post-process" the triangulated surface and remove some vertices. Wyvill et al. [16] also give an algorithm based upon cubes and linear interpolation. They mention the problem of ambiguous faces, but they deal with the triangulation in quite a different manner than it is done here. In order to facilitate the

triangulation of nonplanar polygons, they always append the centroid.

One of the purposes of computing contour surfaces is to provide a means of graphing or visualizing 3D data. Other techniques are discussed by Hamann [8], Foley et al.[5] , Kaufman [9], Upson [14] and Nielson et al.[13].

Acknowledgements

This work was supported by the U.S. Department of Energy under contract DE-FG02-87ER25041 to Arizona State University. We wish to thank the members of the CAGD group at ASU for their help and support. We thank David Lane for providing the image of Figure 18.

References

1. Baker, H., "Computation and manipulation of 3D surfaces from image sequences," in: G. Nielson and B. Shriver (eds.) Visualization in Scientific Computing, IEEE Computer Society Press, Los Alamitos, CA, 1990.

2. Cline, H. E., Lorensen, W. E., Ludke, S., Crawford, C. R., and Teeter, B. C., "Tow algorithms for the reconstruction of surfaces from tomograms," Medical Physics, June 1988.

3. Choi, B. K., Shin, H. Y., Yoon, Y. I., and Lee, J. W., "Triangulation of scattered data in 3D Space," CAD, Vol. 20, No. 5, pp. 239-248.

4. Dürst, M. J., "Letters: Additional reference to "marching cubes"," Computer Graphics, Vol. 22, No.2.

5. Foley, T. A., Lane, D. A., and Nielson, G. M., "Towards animating ray-traced volume visualization," The Journal of Visualization and Computer Animation, Vol. 1, No. 1, 1990, pp. 2-8

6. Franke, R., and Nielson, G. M., "Scattered data interpolation and applications: A tutorial and survey, in *Geometric Modelling: Methods and Their Applications*, H. Hagen & D. Roller (eds.), Springer.

7. Fuchs H., Levoy M., and Pizer S.M., "Interactive Visualization of 3D Medical Data," *Computer*, Vol. 22, No. 8, Aug. 1989, pp. 46-51.

8. Hamann, B., "Visualisierungstechniken zur Darstellung dreidimensionaler Datenmengen," (Techniques for Visualizing Three-dimensional Data Sets, in German), to appear in: CAD Computergraphik, Austria.

9. Kaufman, A. (ed.), Volume Visualization, IEEE Computer Society Press, Los Alamitos, 1990.

10. Lorensen W.E., and Cline H.E., "Marching Cubes: A High-Resolution 3D Surface Construction Algorithm," SIGGRAPH 87 Conference Proceedings, *Computer Graphics*, Vol. 21, No. 4, July 1987, pp. 163-169.

11. Nielson, G. M., and Hamann, B., "Techniques for the interactive visualization of volumetric data," Proceedings of Visualization '90, IEEE Computer Society Press, October, 1990, pp. 45-50.

12. Nielson, G., and Dierks, T. "Modelling and Visualization of Scattered Volumetric Data, SPIE Proceedings Conference 1459, San Jose, February, 1991.

13. Nielson, G. M., Foley, T. A., Hamann, B., and Lane, D. A., "Visualization and modelling of scattered multivariate data, *Computer Graphics and Applications*, May 1991, pp. 47-55.

14. Upson, C. (ed.) , Proceedings of the Chapel Hill Workshop on Volume Visualizaiton, Chapel Hill, NC, May 1989.

15. Wilhelms, J., and Van Gelder, A. "Topological considerations in isosurface generation," *Computer Graphics*, Vol. 24, No. 5, pp. 79-86.

16. Wyvill, G. , Mc Pheeters, C., and Wyvill, B.,Data structures for soft objects," The Visual Computer, Vol. 2, No. 4, pp. 227-234.

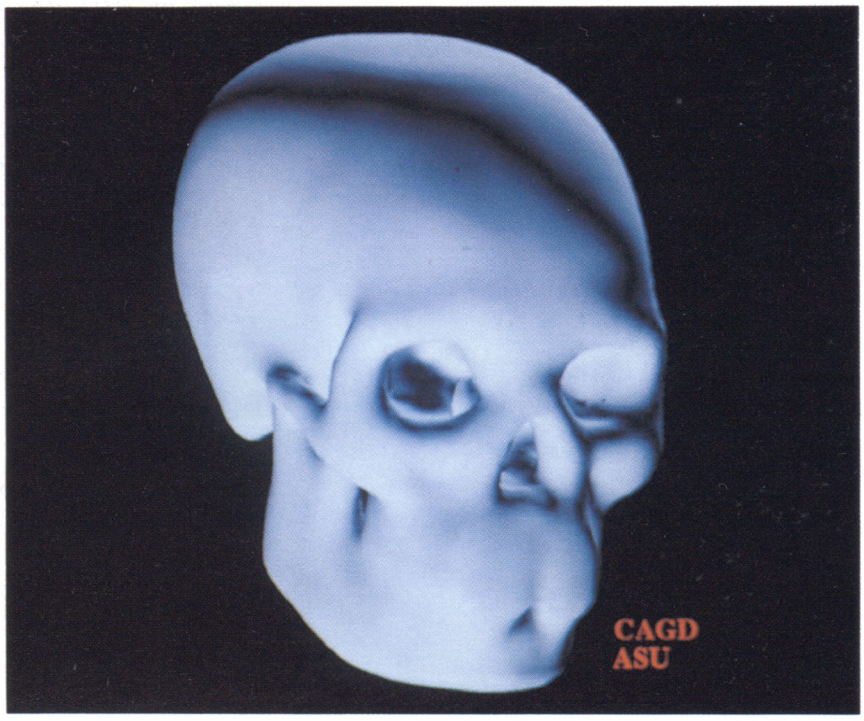

Figure 17. Isovalue surface of skull data.

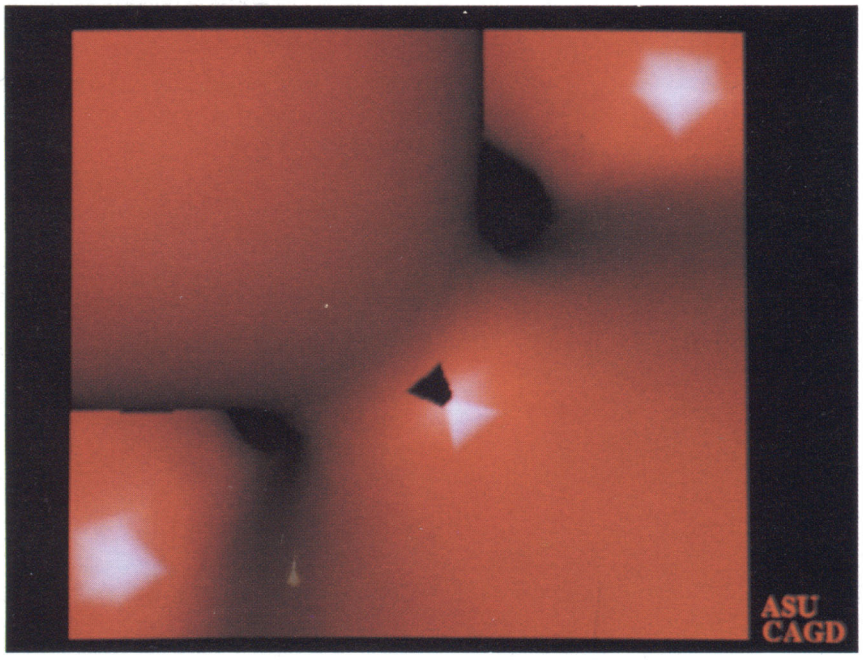

Figure 18. Flaw with mc method.